

Arene C(sp^2)-H Metalation at Ni^{II} modeled with a Reactive PONC_{Ph} Ligand

Linda S. Jongbloed,^a Diego García-López,^b Richard van Heck,^a Maxime A. Siegler,^c Jorge J. Carbó,^b Jarl Ivar van der Vlugt^{*,a}

^a Homogeneous, Bioinspired & Supramolecular Catalysis, van ‘t Hoff Institute for Molecular Sciences, University of Amsterdam, Science Park 904, 1098 XH Amsterdam, the Netherlands. E-mail: *j.i.vandervlugt@uva.nl*

^b Departament de Química Física i Inorgànica, Universitat Rovira i Virgili, Marcel·lí Domingo s/n, 43007 Tarragona, Spain.

^c Department of Chemistry, John Hopkins University, Baltimore MD, United States of America.

Abstract

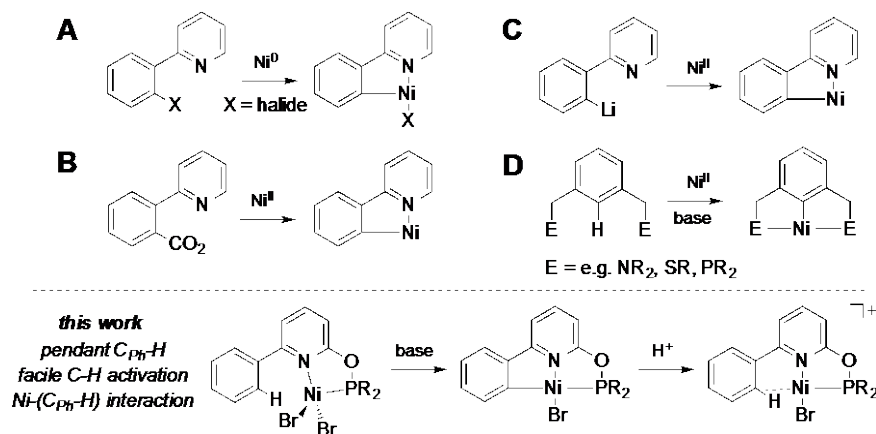
Coordination of the reactive phosphinitopyridylphenyl PONC_{Ph} ligand **L^H** to NiBr₂ initially yields paramagnetic brown NiBr₂(**L^H**) (**1**) but addition of triethylamine results in fast and facile cyclometalation at Ni^{II}, giving NiBr(κ^3 -P,N,C-**L**) (**2**) as well-defined species. This is a rare example of direct cyclometalation at Ni^{II} from a C-H bond in a ligand structure other than encumbering ligands (*e.g.* ECE pincers). Diamagnetic yellow complex **2** reacts instantaneously with HBF₄ to give purple [NiBr(κ^3 -P,N-**L^H**)]BF₄ (**3**). A very unusual anagostic Ni(C_{Ph}-H) interaction in the solid state structure of **3** was unequivocally demonstrated using single crystal X-ray crystallography and was interpret by DFT calculations (QTAIM and ELF analysis). These compounds may be viewed as models for key intermediates in the Ni-catalyzed C-H functionalization of arenes.

Introduction

Catalytic C-H activation is enjoying widespread attention as an efficient and selective methodology for the functionalization of hydrocarbons.¹ Cyclometalation typically precedes the functionalization of aryl C(sp²)-H bonds, using the ligating effect of a neighbouring group to orient the C-H bond within the metal coordination sphere.² Pyridine has proven very efficient as a directing group, and a variety of second- and third-row metal based systems facilitate the selective C-H metalation of pyridylarenes. In stark contrast to its second-row congener Pd, Ni-based systems were very underdeveloped for selective C(sp²)-H functionalization until recently.^{3,4,5,6} For stoichiometric cyclometalation at Ni, the Ni-C bond is generally induced via oxidative addition of a carbon-halogen fragment (to Ni⁰; Scheme 1, **A**),⁷ decarboxylation (**B**)⁸ or transmetalation from a lithiated derivative (**C**).⁹ Formation of a Ni-C bond from an unactivated C-H bond is only common for encumbering ligand structures that enforce the C-H bond in close proximity of the metal, such pincer-type ECE ligands and macrocyclic structures (**D**).¹⁰ For less restricting ligand structures, procedures involving direct C-H metalation pathways with nickel are rare,¹¹ despite the fact that the first reported cyclometalated complex ever reported involves the reaction of nickelocene with azobenzene.¹²

The involvement of a nickelacycle was recently postulated as intermediate for the Ni-catalyzed aromatic C-H bond functionalization, using a bidentate directing-group approach.^{3,4,13} Despite their intermediacy in various catalytic processes, including

ethylene oligo- and polymerization,¹⁴ only few systematic reactivity studies of the Ni–carbon bond in these entities are reported.^{10d,11b,11c} Furthermore, very little information is available on agostic interactions in Ni^{II} complexes, for which the C_{Ar}-H bond interacts with the Ni^{II} center.¹⁵ While this type of bonding most likely precedes the actual C-H activation or metalation step and is therefore an interesting research topic, isolated complexes with agostic interactions are scarcely documented for first-row TM pincer complexes.^{16,17}



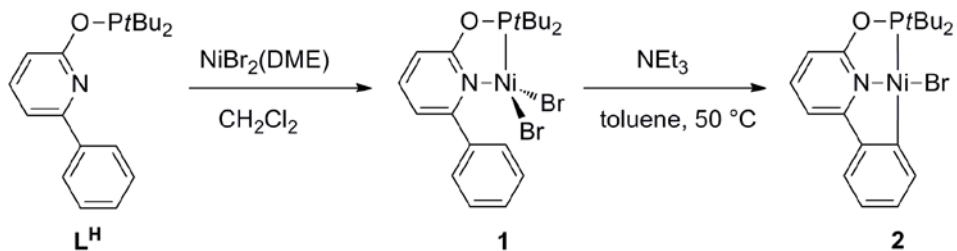
Scheme 1. Well-defined routes A-D toward cyclometalated Ni^{II} species and new direction presented in this work, involving direct cyclometalation of an arene C-H bond.

Motivated by our interest in reactive ligand systems,¹⁸ we recently introduced reversible cyclometalation as strategy for cooperative catalysis, using a strongly chelating *P,N*-ligand that featured a flanking phenyl arm.¹⁹ Expanding on these results, we set out to investigate the potential for cyclometalation and stabilization of an agostic M-(C-H) interaction using the versatile coordination chemistry displayed by ligands of this type.²⁰ Herein we report the fast and facile cyclometalation of the related 2-phosphinito-6-phenyl-pyridine (PONC_{Ph}) ligand **L^H** to Ni^{II}, leading to a complex bearing the cyclometalated phenyl group as a flanking entity. In contrast to

the pivotal phenyl ring found in traditional pincer systems, this side-arm position is more accessible and susceptible to follow-up chemistry. Protonation of the Ni-C bond leads to an example of a structurally characterized $\text{Ni}(\text{C}_{\text{Ph}}\text{-H})$ complex. DFT calculations suggest the existence of a bona fide albeit weak Ni-(C-H) interaction.

Results and Discussion

Synthesis of nickel complexes **1 and **2**.** Reaction of the novel ligand **L^H** with $\text{NiBr}_2(\text{DME})$ at r.t. yielded the brown paramagnetic species $\text{NiBr}_2(\kappa^2\text{-P},\text{N-}\text{L}^{\text{H}})$ **1** (Scheme 2), showing a magnetic moment μ_{eff} of $3.29 \mu_{\text{B}}$ (Evans method).²¹ Species **1** was characterized by single crystal X-ray crystallography (Figure 1, left). The pseudo-tetrahedral geometry around Ni is distorted due to the flanking Ph ring, with $\angle \text{N}_1\text{-Ni}_1\text{-Br}_1$ at $95.71(7)^\circ$ and $\angle \text{N}_1\text{-Ni}_1\text{-Br}_2$ at $144.27(7)^\circ$. The closest Ni-C_{Ph} contact is $\pm 3.0 \text{ \AA}$. Comparable $(\text{P}^{\text{N}})\text{NiX}_2$ complexes show less distortion from tetrahedral geometry and usually give lower values for μ_{eff} . Our value for μ_{eff} corresponds more to values found for bimetallic trigonal bipyramidal structures with bridging chlorides.²² However, magnetic properties for Ni^{II} complexes are highly dependent on the ligand field and large deviations can be found due to structural equilibria in solution.



Scheme 2. Coordination of ligand **L^H** to $\text{Ni}^{\text{II}}\text{Br}_2(\text{DME})$ to paramagnetic **1** and subsequent cyclometalation to complex **2**.

Addition of 10 equiv. of triethylamine to a toluene solution of **1** at 50 °C led to a gradual color change from brown to yellow within 30 minutes, concomitant with appearance of well-defined NMR spectral features for a new species **2**, suggesting a diamagnetic product. The ^{31}P NMR chemical shift at δ 187 ppm (free L^{H} : 153 ppm) and a doublet at δ 156 ppm in the ^{13}C NMR spectrum with a $^2J_{\text{CP}}$ coupling constant of 101 Hz are suggestive of a cyclometalated species. The molecular structure for **2** (Figure 1, right) confirms the selective C-H metalation of the phenyl side-arm of L^{H} to give $\text{NiBr}(\kappa^3\text{-P,N,C-L})$. The $\text{Ni}_1\text{-C}_1$ bond length of 1.9265(49) Å is similar to that observed for other nickelacycles with a flanking phenyl ring, which all fall in the range 1.91-1.95 Å.^{7-9,11} The Ni-C bond in **2** is longer in comparison to related (POCN) NiBr complexes, which have the phenyl ring in the pivotal position and have Ni-C bond lengths of 1.85-1.86 Å.²³ The difference in Ni-C bond lengths indicates the impact of encumbering ligands. The angle $\angle \text{P}_1\text{-Ni}_1\text{-C}_1$ of 166.28(12)° combined with the mutual *trans* disposition of the σ -donating phenyl-fragment and the phosphinite donor might potentially impose enhanced reactivity to the Ni-C fragment.

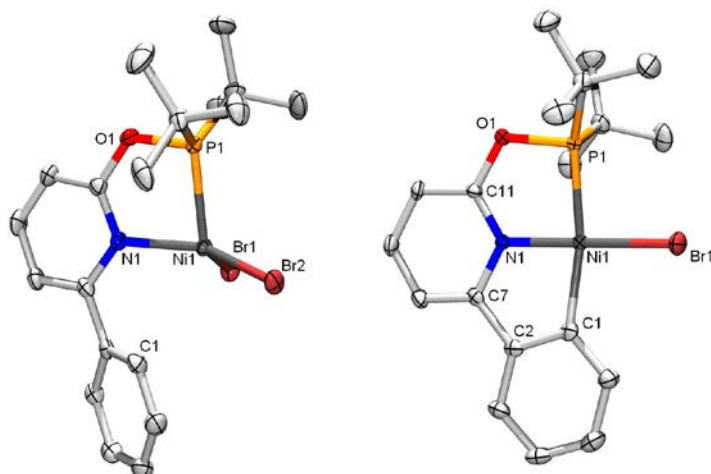
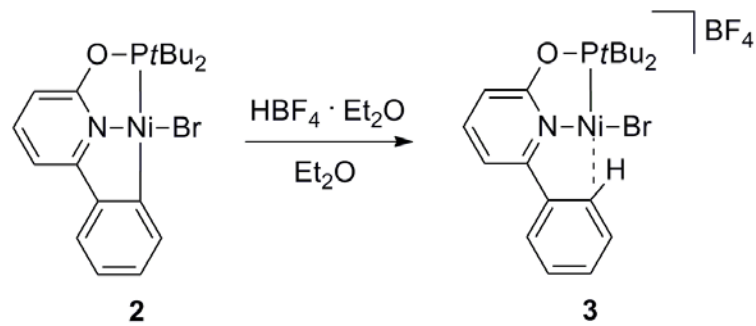


Figure 1. Displacement ellipsoid plots (50% probability level) for **1** (left) and **2** (right) Selected bond lengths (Å) and angles (°), for **1**: $\text{Ni}_1\text{-P}_1$ 2.2859(9); $\text{Ni}_1\text{-N}_1$ 2.075(3); $\text{Ni}_1\text{-Br}_1$ 2.3535(5); $\text{Ni}_1\text{-Br}_2$ 2.3555(5); $\text{Ni}_1\cdots\text{C}_1$ 3.039; $\text{P}_1\text{-Ni}_1\text{-N}_1$ 82.25(9); $\text{P}_1\text{-Ni}_1\text{-Br}_1$ 113.66(4); $\text{P}_1\text{-Ni}_1\text{-Br}_2$ 105.71(3); $\text{N}_1\text{-Ni}_1\text{-Br}_1$ 95.71(7); $\text{N}_1\text{-Ni}_1\text{-Br}_2$ 144.27(7); $\text{Br}_1\text{-Ni}_1\text{-Br}_2$ 111.73(2). For **2**: $\text{Ni}_1\text{-P}_1$ 2.2046(11); $\text{Ni}_1\text{-N}_1$ 1.875(3); $\text{Ni}_1\text{-C}_1$

1.923(4); Ni₁-Br₁ 2.3023(6); P₁-Ni₁-N₁ 82.99(10); P₁-Ni₁-Br₁ 97.25(3); P₁-Ni₁-C₁ 166.28(12); N₁-Ni₁-C₁ 83.91(15); N₁-Ni₁-Br₁ 178.58(10).

Addition of an equimolar amount of ethereal HBF₄ to a yellow toluene solution of **2** (Scheme 3) led to instantaneous precipitation of a purple solid. ESI-MS suggested the formation of a mononuclear cationic species with a reprotonated ligand fragment. In dichloromethane, a band at λ 535 nm (ϵ 1485 L mol⁻¹ cm⁻¹) was observed in the visible region of the UV-vis spectrum, but NMR spectroscopy (³¹P, ¹H or ¹³C) proved ineffective, suggestive of solution-state paramagnetism. Single crystal X-ray diffraction corroborated the solid-state structure of complex **3** to be formulated as [NiBr(κ^3 -P,N,(C-H)-L^H)]BF₄ (Figure 2, left). The molecular structure displays a slightly distorted square planar Ni-center, which has a coordinative interaction with an aromatic C-H bond *ortho* to the pyridine ring (the corresponding proton H₁, which is actually found almost within the arene plane, could be localized in the difference Fourier contour map (Figure 2, right). This interaction was evidenced by the Ni₁…H₁ distance of 2.02(9) Å and the Ni₁…C₁ distance of 2.355(8) Å, which is much shorter than the van der Waals radii (3.3 Å for Ni…C). Furthermore, H₁ is tilted ~10° from the aromatic plane, which is more often observed for complexes with an M-(CH) interaction and can be as large as 35°.^{16,17,20a,24} The Ni₁-P₁, Ni₁-N₁ and Ni₁-Br₁ bonds are slightly contracted relative to **2**. Addition of NEt₃ to a suspension of **3** in toluene at room temperature led to almost instantaneous regeneration of **2**, suggestive of facile deprotonation of the C_{Ph}-H bond in this cationic complex. The closest related structure is from a nickel benzoporphyrin, which shows a Ni…(CH) distance of ~2.4 Å.¹⁶



Scheme 3. Selective protonation of the Ni-C bond in **2** to generate the cationic derivative **3** with a coordinative Ni-(C-H) interaction.

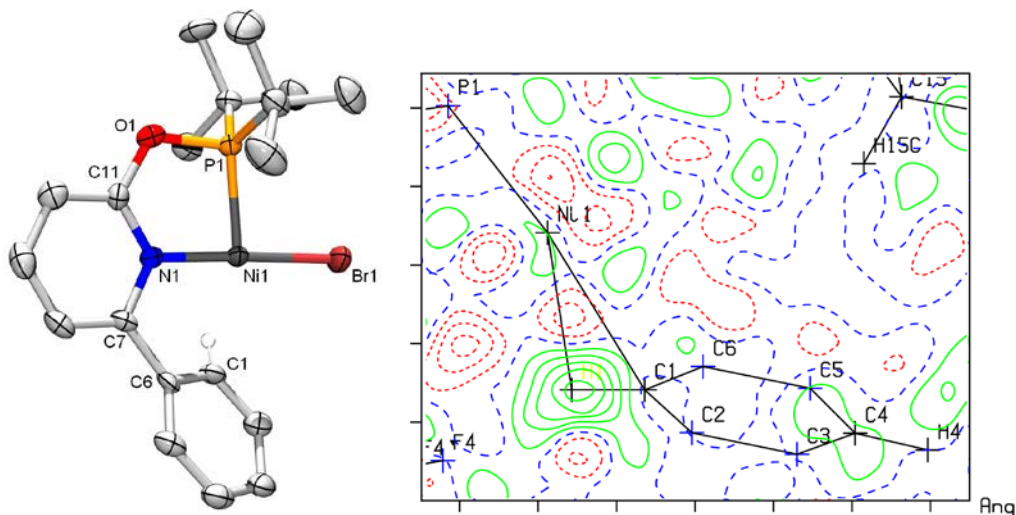


Figure 2. Left: Displacement ellipsoid plot (50% probability level) for the cationic part of **3**. Selected bond lengths (\AA) and angles ($^\circ$) for **3**: $\text{Ni}_1\text{-P}_1$ 2.130(2); $\text{Ni}_1\text{-N}_1$ 1.876(6); $\text{Ni}_1\text{-Br}_1$ 2.2555(12); $\text{Ni}_1\cdots\text{C}_1$ 2.355(8); $\text{Ni}_1\cdots\text{H}_1$ 2.02(9); $\text{P}_1\text{-Ni}_1\text{-N}_1$ 84.75(19); $\text{P}_1\text{-Ni}_1\text{-Br}_1$ 97.34(7); $\text{P}_1\text{-Ni}_1\text{-C}_1$ 163.3(2); $\text{N}_1\text{-Ni}_1\text{-C}_1$ 80.6(3); $\text{N}_1\text{-Ni}_1\text{-Br}_1$ 176.37(19); torsion $\angle\text{C}_1\text{-C}_6\text{-C}_7\text{-N}_1$ -29.7(10); $\angle\text{H}_1\text{-C}_1\text{-C}_2\text{-C}_3$ -169(6). Right: The difference Fourier contour map of complex **3**, which shows the location of H_1 , the proton that contributes to the $\text{C}_1\text{-H}_1\text{-Ni}_1$ interaction.

Intrigued by the observation of the unusual Ni-(C_{Ph} -H) interaction in the solid state, we were motivated to understand the bonding in complex **3** by means of DFT calculations. Therefore, we analyzed the topology of electron density within the quantum theory of atoms in molecules (QTAIM) and the topology of electron localization function (ELF). These methods have recently been exploited to study the

bonding between Rh^I and the C_{Ph}-H fragment of a protonated PCP-pincer.²⁵ These investigations also complement computational work on the nature of intramolecular non-bonding interactions by some of us.²⁶ The solid state structure of **3** is well-reproduced by DFT calculations in the singlet state. The computed relevant metric parameters, i.e. the Ni···C₁ and Ni···H₁ distances (2.364 and 2.094 Å) and the tilting of H₁ from the planar phenyl ring (~10°), are nearly identical to the solid state structure obtained from X-ray diffraction. The C₁-H₁ bond length is elongated with respect to that in the free ligand (from 1.085 to 1.099 Å) and the C₁-H₁ stretching frequency decreases relatively to **L^H** (from 3233 to 3071 cm⁻¹). These observations, along with the H₁ tilting, are indicative of an interaction between nickel and the C-H bond.

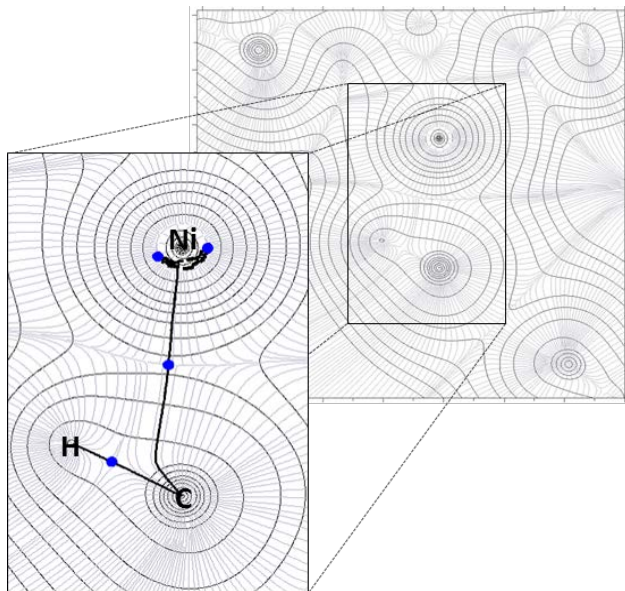
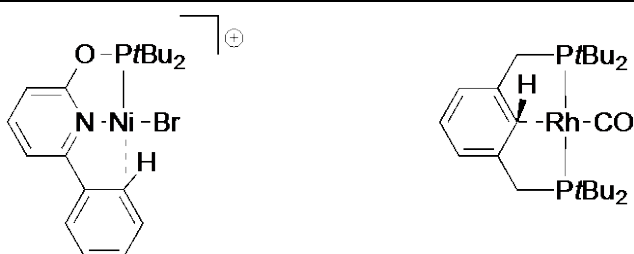


Figure 3. DFT calculated contour map of electron charge density, $\rho(r)$, showing the bond critical point that links the Ni and C₁ atom.

Figure 3 shows the computed density map for a plane that contains Ni and the C_{Ph}-H fragment. One bond critical point (BCP) linking the Ni and C₁ atoms was localized

(indicated by a blue dot). According to QTAIM theory, a chemical bond exists if a line of locally maximum electron density links two neighboring atoms and also if along that line there is a BCP, evidencing in this case a Ni-(η^1 -C₁) interaction. Noteworthy is the curving of the bond path toward H₁, which indicates that two charge density maxima, corresponding to the Ni \cdots H₁ and Ni \cdots C₁ BCPs, and a minimum, corresponding to the ring critical point (RCP), were very closely situated and have collapsed into one maximum. At the BCP, the low value of the electronic charge density, ($\rho(r) = 0.037$) and the low and positive values of the Laplacian of the charge density, ($\nabla^2\rho(r) = 0.167$) are indicative of closed shell-type interaction. Table 1 summarizes the main geometric and spectroscopic parameters, and the results of QTAIM and ELF analysis for complex **3**. Moreover, a direct comparison using the same computational level is made between **3** and [Rh(CO)(PC^HP)]⁺, for which a Rh-(η^1 -C_{Ph}) interaction with a concomitant agostic η^2 -(C,H) interaction was proposed.²⁵

Table 1. Geometric, spectroscopic, energetic, QTAIM and ELF parameters for the M-(C-H) interaction in complex **3** [NiBr(κ^3 -P,N,(C-H)-L^H)]⁺ and the previously reported [Rh(CO)(P(C-H)P)]⁺ complex.²⁵



Distances in Å, angles in deg, and distance ratio

$d(\text{C}\cdots\text{M})$	2.364	2.289
$d(\text{H}\cdots\text{M})$	2.094	2.006
$d(\text{C}-\text{H})$	1.099	1.122
C-H out-of-plane bending	12.6°	14.7°
$d(\text{C}-\text{H}) / d(\text{H}\cdots\text{M})$	0.52	0.56

Vibrational frequencies in cm⁻¹, and frequency ratio		
v(C-H)	3071	2807
v(C-H) / v(C-H _{free L})	0.95	0.88
Electron density, ρ, and Laplacian, ∇²ρ, at the BCP's in a.u.; and ρ_{BCP} ratio		
ρ _{BCP} , ∇ ² ρ _{BCP} (C···M)	0.037, 0.167	0.062, 0.215
ρ _{BCP} , ∇ ² ρ _{BCP} (C-H)	0.272, -0.919	0.254, -0.779
ρ _{BCP} (C-H) / ρ _{BCP} (C-H _{free L})	0.95	0.90
ELF population of valence basins in a.u.		
V(C,M)	0.16	0.31
V(C,H _{agostic})	2.20	2.18

With ELF analysis a disynaptic V(M,C) attractor was found between nickel and aromatic carbon C₁, indicating an electron-sharing interaction between those atoms (Figure 4). This topology is analogous to that reported for [Rh(CO)(PC^HP)]⁺²⁵, however, the population of the V(M,C) basin in **3** (0.16 e) is lower than in cationic [Rh(CO)(PC^HP)]⁺ (0.31 e), suggesting that the bonding situation in **3** is closer to the anagostic η^1 -C interaction.

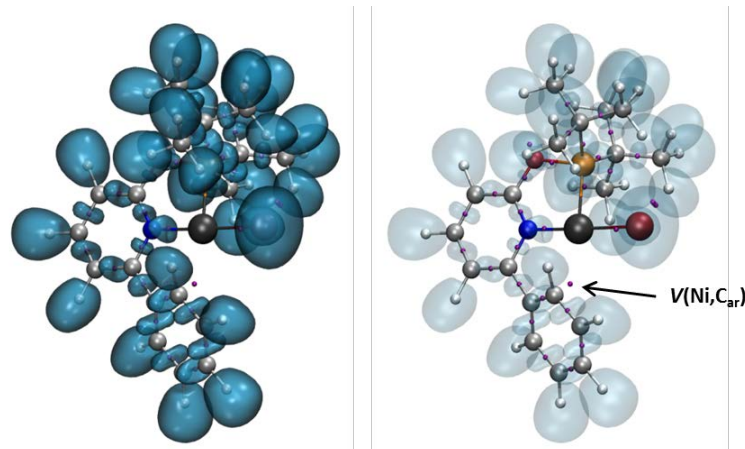


Figure 4. ELF localization domains (ELF = 0.81) for **3** and the disynaptic V(M,C) attractor with a populated basin of 0.16 e.

The procedure to evaluate this type of intramolecular bond strengths is not straightforward. One way to estimate it is by calculating the energy difference of the

structure displaying a Ni-(C-H) interaction and a configuration lacking this binding motif. In this case, we determined the transition state for aryl rotation, in whose structure the aryl ring is perpendicular to the pyridine ring and the its C-H bonds are far away from the Ni. The computed free energy barrier is very low at 4.8 kcal.mol⁻¹, indicating that the (C-H)…Ni interaction is even weaker. This is in agreement with our previous observation for a related Rh-(C_{Ph}-H) complex, showing fast rotation around C_{Ph}-C_{Py} even at -90 °C.^{21a} Alikhani *et al.* recently proposed several criteria based on geometric, spectroscopic and QTAIM parameters to classify the strength of *agostic* bonding as anagostic, weak-to-medium agostic, medium-to-strong agostic or pre-hydride.²⁷ Table 1 includes the three QTAIM normalized parameters that consist of the ratio between the C-H_{agostic} distance and the H_{agostic}…M distance, the ratio between the stretching frequency of C-H_{agostic} bond in the complex and in the free ligand, and the ratio between the electron density at the BCP, ρ_{BCP}, in the complex and in the free ligand. The computed values for complex **3** provide a mixed situation. The geometric parameters fulfill the criteria set for a weak-to-medium agostic C-H interaction (ratio range: 0.5-0.7), but the spectroscopic and topological parameters do not, showing values typical of anagostic bonding (ratio range ≥ 0.90 for both). We therefore tend to favor the description of a Ni-(C_{Ph}-H) interaction in the solid state with predominant Ni-(η¹-C_{Ph}) character.

Conclusions

In conclusion, we have reported the facile base-induced cyclometalation of a pendant phenyl ring within the novel ligand **L^H** to convert NiBr₂(κ²-*P,N*-**L^H**) (**1**) into NiBr(κ³-*P,N,C*-**L**) (**2**). This is a rare example of unrestricted C-H metalation at Ni^{II} under mild

conditions. The PONC_{Ph} framework can thus act as flexidentate ligand in the coordination sphere of Ni^{II}, switching between bi- and tridentate coordination depending on the reaction conditions. The nickel-carbon bond proved to be susceptible to reprotonation with HBF₄, generating the structurally characterized species [NiBr(κ^3 -P,N,(C-H)-L^H)]BF₄ (**3**). The nature of the Ni-(C_{Ph}-H) bond was computationally shown to be a bona fide albeit weak (an)agostic coordinative interaction, with predominant Ni-(η^1 -C_{Ph}) character. Compounds **2** and **3** may be viewed as models for key intermediates in the Ni-catalyzed C-H functionalization of arenes.

Experimental Section

General methods. All reactions were carried out under an atmosphere of nitrogen using standard Schlenk techniques. Reagents were purchased from commercial suppliers and used without further purification. 6-phenyl-2-pyridone was ordered from TCI. THF, pentane, hexane and Et₂O were distilled from sodium benzophenone ketyl. CH₂Cl₂ was distilled from CaH₂, toluene from sodium under nitrogen. NMR spectra (¹H, ¹H{³¹P}, ³¹P, ³¹P{¹H}, ³¹P-¹H and ¹³C{¹H}) were measured on a Bruker DRX500 MHz, a Bruker AV400 or a Bruker AV300 MHz spectrometer. IR spectra (ATR) were recorded with a Bruker Alpha-p FT-IR spectrometer. High resolution mass spectra were recorded on or JMS-T100GCV mass spectrometer using field desorption (FD) or JEOL AccuTOF LC, JMS-T100LP mass spectrometer.

Synthesis and characterization of new compounds

Ligand L^H. To a solution of 6-phenyl-2-pyridone (0.64 g, 3.7 mmol), *N,N,N',N'*-tetramethylethylenediamine (1.1 mL, 7.4 mmol, 2 equiv.) and NEt₃ (1.6 mL, 11.1

mmol, 3 equiv.) in THF (30 mL) was added di-*tert*-butylchlorophosphine (0.74 mL, 3.9 mmol) dropwise after which the mixture was refluxed for 1 week. The solvent was evaporated and the product was extracted with toluene (20 mL), filtered and evaporated to dryness to yield the product as a white oil (1.10 g, 94%). ^1H NMR (CDCl_3 , 298 K, 300 MHz, ppm): δ 8.08 – 8.01 (m, 2H), 7.65 (t, J = 7.8 Hz, 1H), 7.48–7.33 (m, 4H), 6.83 (d, J = 8.1 Hz, 1H), 1.25 (d, $^3J_{\text{HP}} = 11.6$ Hz, 18H). ^{31}P NMR (CDCl_3 , 298 K, 121 MHz, ppm): δ 152.72. ^{13}C NMR (CDCl_3 , 298 K, 75 MHz, ppm): δ 164.54 (d, $^2J_{\text{CP}} = 7.6$ Hz, Py-C), 155.62(s, Py-C), 139.58(s, Py-CH), 139.03 (s, Ph-C), 128.90 (s, Ph-CH), 128.68 (s, 2C, Ph-CH), 127.01 (s, 2C, Ph-CH), 113.94 (s, Py-CH), 110.80 (d, $^3J_{\text{CP}} = 3.2$ Hz, Py-CH), 35.72 (d, $^1J_{\text{CP}} = 27.0$ Hz, PC(CH_3)₃), 27.79 (d, $^2J_{\text{CP}} = 15.7$ Hz, PC(CH_3)₃). HR-MS (ESI): m/z calcd. for $\text{C}_{19}\text{H}_{26}\text{NOP}$: 316.1830 [M+H]⁺; found: 316.1827.

Complex 1, Ni(Br)₂($\kappa^2\text{-P,N-L}^{\text{H}}$). Ligand L^{H} (0.45 g, 1.40 mmol) was dissolved in CH_2Cl_2 (10 mL) and $\text{NiBr}_2(\text{DME})$ (0.42 g, 1.36 mmol) was added. After stirring for 30 min, the solvent was evaporated and the remaining solids are washed with pentane (10 mL). Slow evaporation of a CH_2Cl_2 /pentane solution yielded the brown product (0.54 g, 74%) and crystals suitable for X-ray analysis. Effective magnetic susceptibility $\mu_{\text{eff}} = 3.29 \mu_{\text{B}}$ (Evans method). HR-MS (ESI): m/z calcd. for $\text{C}_{19}\text{H}_{26}\text{BrNNiOP}$: 454.0263 [M-Br]⁺; found: 454.0245. UV-Vis (CH_2Cl_2 , nm): λ 294 ($\epsilon = 1.3 \times 10^4 \text{ L} \cdot \text{mol}^{-1} \cdot \text{cm}^{-1}$), λ 344 ($\epsilon = 3.6 \times 10^3 \text{ L} \cdot \text{mol}^{-1} \cdot \text{cm}^{-1}$), λ 400 ($\epsilon = 1.6 \times 10^3 \text{ L} \cdot \text{mol}^{-1} \cdot \text{cm}^{-1}$), λ 513 ($\epsilon = 1.9 \times 10^2 \text{ L} \cdot \text{mol}^{-1} \cdot \text{cm}^{-1}$). Elemental analysis (%): calcd for $\text{C}_{19}\text{H}_{26}\text{Br}_2\text{NNiOP}$: C 42.74, H 4.91, N 2.62; found C 42.75, H 4.89, N 2.59.

Complex 2, Ni(κ^3 -P,N,C-L)(Br). Ligand **L^H** (0.57 g, 1.8 mmol) was dissolved in CH₂Cl₂ (6 mL) and NiBr₂(DME) (0.53 g, 1.7 mmol) was added. After stirring for 30 min, the solvent was evaporated and the remaining solids are washed with pentane (10 mL). Toluene (30 ml) and NEt₃ (2.4 mL, 17 mmol, 10 equiv.) are added and the mixture is stirred at 50 °C for 1 hour. After cooling, toluene is evaporated and the yellow product is extracted with Et₂O (60 ml) to yield analytically pure **2** (0.59 g, 72%). Crystals suitable for X-ray diffraction were grown by layering with THF/pentane. ¹H NMR (MeCN-*d*₃, 298 K, 300 MHz, ppm): δ 7.90 (ddd, *J* = 8.4, 7.8, 0.8 Hz, 1H, Py-CH), 7.80 (m, 1H, Ph-CH), 7.44 (m, 1H, Ph-CH), 7.36 (dd, *J* = 7.7, 1.0 Hz, 1H, Py-CH), 7.20–7.08 (m, 2H, Ph-CH), 6.85 (dd, *J* = 8.2, 1.0 Hz, 1H, Py-CH), 1.56 (d, ³*J*_{HP} = 14.2 Hz, 18H). ³¹P NMR (MeCN-*d*₃, 298 K, 121 MHz, ppm): δ 187.05. ¹³C NMR (MeCN-*d*₃, 298 K, 75 MHz, ppm): δ 166.42 (d, *J*_{CP} = 4.6 Hz, Py-C), 164.84 (d, *J*_{CP} = 9.9 Hz, Py-C), 155.94 (d, ²*J*_{CP} = 101.0 Hz, Ni-C), 147.67 (s, Ph-C), 142.79 (s, Py-CH), 137.04 (s, Ph-CH), 129.70 (d, *J*_{CP} = 6.0 Hz, Ph-CH), 125.29 (s, Ph-CH), 122.25 (d, *J*_{CP} = 4.0 Hz, Ph-CH), 111.72 (s, Py-CH), 107.27 (d, ³*J*_{CP} = 4.0 Hz, Py-CH), 38.65 (d, ¹*J*_{CP} = 3.2 Hz, PC(CH₃)₃), 26.73 (d, ²*J*_{CP} = 6.0 Hz, PC(CH₃)₃). HR-MS (FD): *m/z* calcd for C₁₉H₂₅⁸¹BrNNiOP: 453.01901 [M]⁺; found: 453.01918. UV-Vis (MeCN, nm): λ 241 (ϵ = 2.2×10⁴ L·mol⁻¹·cm⁻¹), λ 270 (ϵ = 3.3×10⁴ L·mol⁻¹·cm⁻¹), λ 399 (ϵ = 9.1×10³ L·mol⁻¹·cm⁻¹). Elemental analysis (%): calcd for C₁₉H₂₅BrNNiOP: C 50.38, H 5.56, N 3.09; found C 50.58, H 5.79, N 3.01.

Complex 3, [Ni(κ^3 -P,N,(C-H)-L^H)(Br)]BF₄. Complex **2** (30 mg, 0.066 mmol) was dissolved in Et₂O (5 mL) and 1 equiv. of HBF₄ · Et₂O (9 μL, 0.066 mmol) was added slowly. The purple product precipitates directly and the remaining Et₂O is removed by syringe. The product is washed with Et₂O (3 mL) and is crystallized by layering with

CD_2Cl_2 /pentane. Despite several attempts the product could never be obtained as pure bulk material, due to the unstable nature of the product (even in crystalline form). However, some pure crystalline material could be separated by hand picking; this material was used for X-ray crystallographic analysis, MS analysis and UV-Vis spectroscopy. HR-MS (ESI): m/z calcd for $\text{C}_{19}\text{H}_{26}^{81}\text{BrNNiOP}$: 454.02684 [M]⁺, found: 454.02973. UV-Vis (CH_2Cl_2 , nm): λ 243 ($\varepsilon = 2.2 \times 10^4 \text{ L} \cdot \text{mol}^{-1} \cdot \text{cm}^{-1}$), λ 297 ($\varepsilon = 1.3 \times 10^4 \text{ L} \cdot \text{mol}^{-1} \cdot \text{cm}^{-1}$), λ 535 ($\varepsilon = 1.5 \times 10^3 \text{ L} \cdot \text{mol}^{-1} \cdot \text{cm}^{-1}$). Elemental analysis (%): calcd for $\text{C}_{19}\text{H}_{26}\text{BBrF}_4\text{NNiOP}$: C 42.20, H 4.85, N 2.59; found C 41.15, H 5.08, N 2.34. Despite several attempts, this was the most accurate value found for complex **3**, due to the unstable nature of the crystalline material.

DFT calculations and QTAIM/ELF analysis

Geometry optimizations and wave function generation for analysis were performed with Gaussian09 series of programs.²⁸ We optimized $[\text{NiBr}(\kappa^3\text{-P},\text{N},(\text{C}-\text{H})\text{-L}^\text{H})]^+$ structure, and for comparison we computed a Rh(I)-P(CH)P pincer complex exhibiting a Rh- $\eta^1\text{-C}$ bonding with concomitant α -agostic $\eta^2(\text{C},\text{H})$ bonding at the same level of Ni complex (see Table S1). The nature of the minima and transition state stationary points encountered was characterized by means of harmonic vibrational frequencies analysis. Full quantum mechanical calculations were performed within the framework of Density Functional Theory (DFT)²⁹ by using the B3PW91 functional.³⁰ The basis set for Ni, Rh, Br and P atoms was that associated with a pseudopotential,³¹ with a standard double- ξ LANL2DZ contraction, and the basis set was supplemented by f and d shells, respectively.³² The rest of atoms were described with a standard 6-31G(d,p) basis set.³³ The MULTWFn software³⁴ was used for the topological analysis of electron density within the *quantum theory atoms*

in molecules (QTAIM),³⁵ and for the topological analysis of the electron localization function (ELF).³⁶ In the theory of QTAIM, the value of the electron density (ρ_{BCP}) and the Laplacian of electron density ($\nabla^2\rho_{\text{BCP}}$) are used to define the interactions presented in the molecules. For covalent interactions, the ρ_{BCP} and $\nabla^2\rho_{\text{BCP}}$ are high and negative at the BCP, while for the closed-shell interactions own a small value of ρ_{BCP} and a positive $\nabla^2\rho_{\text{BCP}}$.

CCDC 1455563-1455565 contain the supplementary crystallographic data for this paper. These data can be obtained free of charge from The Cambridge Crystallographic Data Centre via www.ccdc.cam.ac.uk/data_request/cif. See SI for crystallographic details.

Acknowledgements

This work was funded by the European Research Council (ERC, Starting Grant 279097, *EuReCat* to J.I.v.d.V.) and by the Spanish Ministerio de Economía y Competitividad (CTQ2014-52774-P) and by the Generalitat de Catalunya (2014SGR199). We thank prof's Joost Reek and Bas de Bruin (UvA) for useful discussions and general interest in our work.

References

- (1) (a) Lyons, T. W.; Sanford, M. S. *Chem. Rev.* **2010**, *110*, 1147-1169. (b) Colby, D. A.; Bergman, R. G.; Ellman, J. A. *Chem. Rev.* **2010**, *110*, 624–655. (c) Wencel-Delord, J.; Dröge, T.; Liu, F.; Glorius, F. *Chem. Soc. Rev.* **2011**, *40*, 4740-4761. (d) Song, G.; Wang F.; Li, X. *Chem. Soc. Rev.* **2012**, *41*, 3651-3678. (e) Arockiam, P. B.; Bruneau, C.; Dixneuf, P. *Chem. Rev.* **2012**, *112*, 5879-5918. (f) Yamaguchi, J.; Itami, K.; Yamaguchi, A. D. *Angew. Chem. Int. Ed.* **2012**, *51*,

- 8960-9009. (g) Rouquet, G.; Chatani, N. *Angew. Chem. Int. Ed.* **2013**, *52*, 11726-11743. (h) Ackermann, L. *Acc. Chem. Res.* **2014**, *47*, 281-295. (i) Huang, Z.; Lim, H. N.; Mo, F.; Young, M. C.; Dong, G. *Chem. Soc. Rev.* **2015**, *44*, 7764-7786. (j) Yang, L.; Huang, H. *Chem. Rev.* **2015**, *115*, 3468-3517. (k) Cheng, C.; Hartwig, J. F. *Chem. Rev.* **2015**, *115*, 8946-8975.
- (2) Albrecht, M. *Chem. Rev.* **2010**, *110*, 576-623.
- (3) (a) Shiota, H.; Ano, Y.; Aihara, Y.; Fukumoto, Y.; Chatani, N. *J. Am. Chem. Soc.* **2011**, *133*, 14952-14955. (b) Aihara, Y.; Chatani, N. *J. Am. Chem. Soc.* **2013**, *135*, 5308-5311. (c) Aihara, Y.; Tobisu, M.; Fukumoto, Y.; Chatani, N. *J. Am. Chem. Soc.* **2014**, *136*, 15509-15512.
- (4) (a) Ruan, Z.; Lackner, S.; Ackermann, L. *Angew. Chem. Int. Ed.* **2016**, *55*, 3153-3157. (b) Song, W.; Lackner, S.; Ackermann, L. *Angew. Chem. Int. Ed.* **2014**, *53*, 2477-2480.
- (5) (a) Cong, X.; Li, Y.; Wei, Y.; Zeng, X. *Org. Lett.* **2014**, *16*, 3926-3929. (b) Ye, X.; Petersen, J. L.; Shi, X. *Chem. Commun.* **2015**, *51*, 7863-7866. (c) Yan, S.-Y.; Liu, Y.-J.; Liu, B.; Liu, Y.-H.; Shi, B.-F. *Chem. Commun.* **2015**, *51*, 4069- 4072. (d) Yang, K.; Wang, Y.; Chen, X.; Kadi, A. A.; Fun, H.-K.; Sun, H.; Zhang, Y.; Lu, H. *Chem. Commun.* **2015**, *51*, 3582- 3585. (e) Barsu, N.; Kalsi, D.; Sundararaju, B. *Chem. Eur. J.* **2015**, *21*, 9364-9368. (f) Yi, J.; Yang, L.; Xia, C.; Li, F. *J. Org. Chem.* **2015**, *80*, 6213-6221. (g) Yan, Q.; Chen, Z.; Yu, W.; Yin, H.; Liu, Z.; Zhang, Y. *Org. Lett.* **2015**, *17*, 2482-2485. (h) Ogata, K.; Atsuumi, Y.; Shimada, D.; Fukuzawa, S.-I. *Angew. Chem. Int. Ed.* **2011**, *50*, 5896-5899.
- (6) For investigations on potential Ni(IV) intermediates, see: (a) Camasso, N. M.; Sanford, M. S. *Science* **2015**, *347*, 1218-1220. (b) Bour, J. R.; Camasso, N. M.; Sanford, M. S. *J. Am. Chem. Soc.* **2015**, *137*, 8034-8037.
- (7) (a) Klein, A.; Rausch, B.; Kaiser, A.; Vogt, N.; Krest, A. *J. Organomet. Chem.* **2014**, *774*, 86-93. (b) Higgs, A. T.; Zinn, P. J.; Sanford, M. S. *Organometallics* **2010**, *29*, 5446-5449. (c) Higgs, A. T.; Zinn, P. J.; Simmons, S. J.; Sanford, M. S. *Organometallics* **2009**, *28*, 6142-6144. (d) Ruhland, K.; Obenhuber, A.; Hoffmann, S. D. *Organometallics* **2008**, *27*, 3482-3495. (e) Ceder, R. M.; Granell, J.; Muller, G. *J. Chem. Soc., Dalton Trans.* **1998**, 1047- 1051. (f) Ceder, R. M.; Granell, J.; Muller, G.; Font-Bardía, M.; Solans, X. *Organometallics* **1996**, *15*, 4618-4624. (g) Ceder, R. M.; Granell, J.; Muller, G.; Font-Bardía, M.; Solans, X. *Organometallics* **1995**, *14*, 5544-

5551. (h) Muller, G.; Panyella, D.; Rocamora, M.; Sales, J.; Font-Bardía, M.; Solans, X. *J. Chem. Soc., Dalton Trans.* **1993**, 2959-2967.
- (8) Cookson, P. G.; Deacon, G. B. *J. Organomet. Chem.* **1971**, 33, C38-C40.
- (9) Zhang, Q.; Zhang, X.-Q.; Wang, Z.-X. *Dalton Trans.* **2012**, 41, 10453-10464.
- (10) (a) Zargarian, D.; Castonguay, A.; Spasyuk, D. M. *Top. Organomet. Chem.* **2013**, 40, 131-174. (b) Stępień, M.; Latos-Grażyński, L.; Szterenberg, L. *Inorg. Chem.* **2004**, 43, 6654-6662. (c) Sripathongak, S.; Barone, N.; Ziegler, C. *J. Chem. Commun.* **2009**, 4584-4586. (d) Yang, C.; Wu, W.-D.; Zhao, L.; Wang, M.-X. *Organometallics* **2015**, 34, 5167-5174.
- (11) (a) Volpe, E. C.; Chadeayne, A. R.; Wolczanski, P. T.; Lobkovsky, E. B. *J. Organomet. Chem.* **2007**, 692, 4774-4783. (b) Vabre, B.; Deschamps, F.; Zargarian, D. *Organometallics* **2014**, 33, 6623-6632. (c) Morrell, D. G.; Kochi, J. K. *J. Am. Chem. Soc.* **1975**, 97, 7262-7270. (d) Tsybizova, A.; Rulíšek, L.; Schröder, D.; Rokob, T. A. *J. Phys. Chem. A* **2013**, 117, 1171- 1180. (e) Wei, Y.; Petronilho, A.; Mueller-Bunz, H.; Albrecht, M. *Organometallics* **2014**, 33, 5834-5844.
- (12) Kleiman, J. P.; Dubeck, M. *J. Am. Chem. Soc.* **1963**, 85, 1544–1545.
- (13) (a) Xu, Z.-Y.; Jiang, Y.-Y.; Yu, H. Z.; Fu, Y. *Chem. Asian J.* **2015**, 10, 2479-2483. (b) Tang, H.; Huang, X.-R.; Yao, J.; Chen, H. *J. Org. Chem.* **2015**, 80, 4672-4682. (c) Castro, L. C. M.; Chatani, N. *Chem. Lett.* **2015**, 44, 410-421.
- (14) Boulens, P.; Pellier, E.; Jeanneau, E.; Reek, J. N. H.; Olivier-Bourbigou, H.; Breuil, P.-A. R. *Organometallics* **2015**, 34, 1139–1142.
- (15) Brookhart, M.; Green, M. L. H.; Parkin, G. *Proc. Natl. Acad. Sci. U.S.A.* **2007**, 104, 6908–6914.
- (16) Stępień, M.; Latos-Grażyński, L.; Szterenberg, L.; Panek, J.; Latajka, Z. *J. Am. Chem. Soc.* **2004**, 126, 4566-4580.
- (17) Murugesan, S.; Stöger, B.; Pittenauer, E.; Allmaier, G.; Veiros, L. F.; Kirchner, K. *Angew. Chem. Int. Ed.* **2016**, 55, 3045-3048.
- (18) Reviews: (a) Khusnutdinova, J. R.; Milstein, D. *Angew. Chem. Int. Ed.* **2015**, 54, 12236-12273. (b) Broere, D. L. J.; Plessius, R.; van der Vlugt, J. I. *Chem. Soc. Rev.* **2015**, 44, 6886-6915. (c) Morris, R. H. *Acc. Chem. Res.* **2015**, 48, 1494–1502. (d) Kuwata, S.; Ikariya, T. *Chem. Commun.* **2014**, 50, 14290-14300. (e) van der Vlugt, J. I. *Eur. J. Inorg. Chem.* **2012**, 363-375. (f) Gunanathan, C.; Milstein, D. *Acc. Chem. Res.* **2011**, 44, 588-602. (g) van der Vlugt, J. I.; Reek, J. N. H. *Angew. Chem. Int. Ed.* **2009**, 48, 8832-8846. Recent examples from our group: (h) Bauer, R. C.;

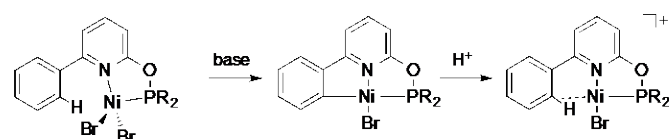
- Gloaguen, Y.; Lutz, M.; Reek, J. N. H.; de Bruin, B.; van der Vlugt, J. I. *Dalton Trans.* **2011**, *40*, 8822-8829. (i) van der Vlugt, J. I.; Pidko, E. A.; Bauer, R. C.; Gloaguen, Y.; Rong, M. K.; Lutz, M. *Chem. Eur. J.* **2011**, *17*, 3850-3854. (j) de Boer, S. Y.; Gloaguen, Y.; Reek, J. N. H.; Lutz, M.; van der Vlugt, J. I. *Dalton Trans.* **2012**, *41*, 11276-11283. (k) Gloaguen, Y.; Jacobs, W.; de Bruin, B.; Lutz, M.; van der Vlugt, J. I. *Inorg. Chem.* **2013**, *52*, 1682-1684. (l) Broere, D. L. J.; de Bruin, B.; Reek, J. N. H.; Lutz, M.; Dechert, S.; van der Vlugt, J. I. *J. Am. Chem. Soc.* **2014**, *136*, 11574-11577. (m) Broere, D. L. J.; Metz, L. L.; de Bruin, B.; Reek, J. N. H.; Siegler, M. A.; van der Vlugt, J. I. *Angew. Chem. Int. Ed.* **2015**, *54*, 1516-1520. (n) Vreeken, V.; Siegler, M. A.; de Bruin, B.; Reek, J. N. H.; Lutz, M.; van der Vlugt, J. I. *Angew. Chem. Int. Ed.* **2015**, *54*, 7055-7059.
- (19) Jongbloed, L. S.; de Bruin, B.; Reek, J. N. H.; Lutz, M.; van der Vlugt, J. I. *Catal. Sci. Technol.* **2016**, *6*, 1320-1328.
- (20) (a) Jongbloed, L. S.; de Bruin, B.; Reek, J. N. H.; Lutz, M.; J. I. van der Vlugt, *Chem. Eur. J.* **2015**, *21*, 7297-7305. See also: (b) Gloaguen, Y.; Jongens, L. J.; Reek, J. N. H.; Lutz, M.; de Bruin, B.; van der Vlugt, J. I. *Organometallics* **2013**, *32*, 4284-4291. (c) Oldenhof, S.; Terrade, F. G.; Lutz, M.; van der Vlugt, J. I.; Reek, J. N. H. *Organometallics* **2015**, *34*, 3209-3215.
- (21) (a) Evans, D. F. *J. Chem. Soc.* **1959**, 2003-2005. (b) Sur, S. K. *J. Magn. Reson.* **1989**, *82*, 169-173. (c) Grant, D. H. *J. Chem. Educ.* **1995**, *72*, 39-40.
- (22) (a) Flapper, J.; Kooijman, H.; Lutz, M.; Spek, A. L.; van Leeuwen, P. W. N. M.; Elsevier, C. J.; Kamer, P. C. J. *Organometallics* **2009**, *28*, 1180-1192. (b) Speiser, F.; Braunstein, P.; Saussine, L.; Welter, R. *Organometallics* **2004**, *23*, 2613-2624. (c) Speiser, F.; Braunstein, P.; Saussine, L. *Organometallics* **2004**, *23*, 2625-2632. (d) Speiser, F.; Braunstein, P.; Saussine, L. *Organometallics* **2004**, *23*, 2633-2640.
- (23) (a) Spasyuk, D. M.; Zargarian, D.; van der Est, A. *Organometallics* **2009**, *28*, 6531-6540. (b) Spasyuk, D. M.; Zargarian, D. *Inorg. Chem.* **2010**, *49*, 6203-6213. (c) Zhang, B.-S.; Wang, W.; Shao, D.-D.; Hao, X.-Q.; Gong, J.-F.; Song, M.-P. *Organometallics* **2010**, *29*, 2579-2587. (d) Mougang-Soumé, B.; Belanger-Gariépy, F.; Zargarian, D. *Organometallics* **2014**, *33*, 5990-6002.
- (24) (a) Vigalok, A.; Uzan, O.; Shimon, L. J. W.; Ben-David, Y.; Martin, J. M. L.; Milstein, D. *J. Am. Chem. Soc.* **1998**, *120*, 12539-12544. (b) Frech, C. M.; Shimon, L. J. W.; Milstein, D. *Organometallics* **2009**, *28*, 1900-1908. (c) Dani, P.; Toorneman, M. A. M.; van Klink, G. P. M.; van Koten, G. *Organometallics* **2000**, *19*, 5287-5296.

- (d) Gusev, D. G.; Madott, M.; Dolgushin, F. M.; Lyssenko, K. A.; Antipin, M. Y. *Organometallics* **2000**, *19*, 1734-1739.
- (25) (a) Lepetit, C.; Poater, J.; Alikhani, M. E.; Silvi, B.; Canac, Y.; Contreras-García, J.; Solà, M.; Chauvin, R. *Inorg. Chem.* **2015**, *54*, 2960-2969. (b) Barthes, C., Lepetit, C., Canac, Y., Duhayon, C., Zargarian, D.; Chauvin, R. *Inorg. Chem.* **2013**, *52*, 48-58.
- (26) (a) Serrano, E.; Navarro, R.; Soler, T.; Carbó, J. J.; Lledós, A.; Urriolabeitia, E. P. *Inorg. Chem.* **2009**, *48*, 6823-6834. (b) Serrano, E.; Vallés, C.; Carbó, J. J.; Lledós, A.; Soler, T.; Navarro, R.; Urriolabeitia, E. P. *Organometallics* **2006**, *25*, 4653-4664. (c) Lledós, A.; Carbó, J. J.; Urriolabeitia, E. P. *Inorg. Chem.* **2001**, *40*, 4913-4917.
- (27) Zins, E.-L.; Silvi, B.; Alikhani, M. E. *Phys. Chem. Chem. Phys.* **2015**, *17*, 9258-9281.
- (28) Frisch, M. J.; Trucks, G. W.; Schlegel, H. B.; Scuseria, G. E.; Robb, M. A.; Cheeseman, J. R.; Scalmani, G.; Barone, V.; Mennucci, B.; Petersson, G. A.; Nakatsuji, H.; Caricato, M.; Li, X.; Hratchian, H. P.; Izmaylov, A. F.; Bloino, J.; Zheng, G.; Sonnenberg, J. L.; Hada, M.; Ehara, M.; Toyota, K.; Fukuda, R.; Hasegawa, J.; Ishida, M.; Nakajima, T.; Honda, Y.; Kitao, O.; Nakai, H.; Vreven, T.; Montgomery Jr., J. A.; Peralta, J. E.; Ogliaro, F.; Bearpark, M.; Heyd, J. J.; Brothers, E.; Kudin, K. N.; Staroverov, V. N.; Kobayashi, R.; Normand, J.; Raghavachari, K.; Rendell, A.; Burant, J. C.; Iyengar, S. S.; Tomasi, J.; Cossi, M.; Rega, N.; Millam, J. M.; Klene, M.; Knox, J. E.; Cross, J. B.; Bakken, V.; Adamo, C.; Jaramillo, J.; Gomperts, R.; Stratmann, R. E.; Yazyev, O.; Austin, A. J.; Cammi, R.; Pomelli, C.; Ochterski, J. W.; Martin, R. L.; Morokuma, K.; Zakrzewski, V. G.; Voth, G. A.; Salvador, P.; Dannenberg, J. J.; Dapprich, S.; Daniels, A. D.; Farkas, O.; Foresman, J. B.; Ortiz, J. V.; Cioslowski, J.; Fox, D. J. *Gaussian 09, Revision A.02*; Gaussian, Inc., Wallingford, CT, 2009.
- (29) Parr, R. G.; Yang, W. in *Density Functional Theory of Atoms and Molecule*, Oxford University Press, Oxford, UK, 1989.
- (30) (a) Becke, A. D. *Phys. Rev. A* **1988**, *38*, 3098-3100. (b) Becke, A. D. *J. Chem. Phys.* **1996**, *104*, 1040-1046. (c) Perdew, J. P. in *Electronic Structure of Solids '91*. Eds.: Ziesche, P.; Eschig, H. Akademie Verlag: Berlin, Germany, **1991**, pp. 11-20.
- (31) Hay, P. J.; Wadt, W. R. *J. Chem. Phys.* **1985**, *82*, 299-310.

- (32) (a) Höllwarth, A.; Böhme, M.; Dapprich, S.; Ehlers, A.W.; Gobbi, A.; Jonas, V.; Köhler, K. F.; Stegmann, R.; Veldkamp, A.; Frenking, G. *Chem. Phys. Lett.*, **1993**, *208*, 237-240. (b) Ehlers, A. W.; Böhme, M.; Dapprich, S.; Gobbi, A.; Höllwarth, A.; Jonas, V.; Köhler, K. F.; Stegmann, R.; Veldkamp, A.; Frenking, G. *Chem. Phys. Lett.*, **1993**, *208*, 111-114.
- (33) (a) Francil, M. M.; Pietro, W. J.; Hehre, W. J.; Binkley, J. S.; Gordon, M. S.; Defrees, D. J.; Pople, J. A. *J. Chem. Phys.* **1982**, *77*, 3654-3665. (b) Hehre, W. J.; Ditchfield, R.; Pople, J. A. *J. Chem. Phys.* **1972**, *56*, 2257-2261. (c) Hariharan, P. C.; Pople, J. A. *Theor. Chim. Acta* **1973**, *28*, 213-222.
- (34) Lu, T.; Chen, F. *J. Comput. Chem.* **2012**, *33*, 580–592.
- (35) Bader, R. F. W. *Chem. Rev.* **1991**, *91*, 893-928.
- (36) Becke, A. D.; Edgecombe, K. E. *J. Chem. Phys.* **1990**, *92*, 5397–5403.
- (37) Bruker, *APEX2* software, Madison WI, USA, 2014.
- (38) Sheldrick, G. M. *SADABS*, Universität Göttingen, Germany, 2008.
- (39) Sheldrick, G. M. *SHELXL2013*, University of Göttingen, Germany, 2013.

For Table of Contents only

Facile direct cyclometalation of a C(sp²)-H bond of a flanking phenyl group in a novel pyridine-phosphinite ligand at Ni^{II} generates a reactive tridentate PONC_{Ph} ligand. Protonation of the nickel-carbon bond affords a Ni-(C_{Ph}-H) interaction in the solid state. The bonding situation is investigated using DFT computations with both QTAIM and ELF methods. Both the nickelacyclic precursor and the Ni-(C_{Ph}-H) species can be considered models for key intermediates in Ni-catalyzed C-H functionalization of arenes.



facile C-H activation of pendant C_{Ph}-H and subsequent Ni-(C_{Ph}-H) interaction by protonation of Ni-C